BI-3

The Analysis of Fracture Surfaces by Electron Microscopy

by Regis M. N. Pelloux* and J. C. McMillan**

The fracture surfaces of metals and alloys exhibit markings and a topography which are characteristic of the mechanisms of fracture operating during the initiation and the propagation of the crack. These markings can be easily and best differentiated by electron microscopy.

This paper reviews and illustrates the characteristic fracture features of the following fracture paths:

Transgranular fracture which can take place either:

- by cleavage or by corrosion along crystallographic planes,
- or by the formation and coalescence of microvoids which leave concave depressions called "dimples" on both fracture surfaces,
- or by the slow progression of a fatigue crack.

Intergranular fracture, which is either:

- brittle when there is a perfect separation of the grains along the grain boundaries,
- or ductile when this separation is associated with the plastic formation of voids along the grain boundaries.

---

* Chief, Materials and Processes, Turbine Division, THE BOEING COMPANY
** Research Engineer, Commercial Airplane Division, THE BOEING COMPANY

I. INTRODUCTION

The word fractography was coined twenty years ago by Zapffe and Clogg. (1) Fractography is the micrographic study of the characteristic features of fracture surfaces. The aim of fractography is to analyze and clarify the fracture features and to attempt to relate the topography of the fracture surface to the causes and basic mechanisms of fracture. A powerful means of investigation has recently been added to the fractography techniques with the use of the electron microscope. Electron micrography is used in the form of a special technique which is called "electron fractography".

The low depth of field (0.2 microns) of the optical microscope makes photomicrography of non-planar surfaces almost impossible. The electron microscope with a considerably larger depth of field, a high resolving power and a large range of magnifications is an ideal tool to study deformed and fractured surfaces. The large depth of field of the electron microscope also makes possible the recording of stereoscopic view which are very helpful in understanding the microscopic topography of a fracture surface.* A complete evaluation of the fracture path and fracture features requires a basic knowledge of the different mechanisms of fracture and also some information on the nature and microstructure of the material. In the case of test specimens, the knowledge of testing variables such as temperature, load, stress at the tip of the crack, stress conditions (plane stress or plane strain), strain rate, environment, etc., help considerably in understanding the microfeatures of the fracture surfaces. In the investigation of a service failure most of these variables will not be known; however, it is always possible to compare the features observed to similar features present on fracture surfaces of the same material tested under known conditions.

This paper reviews and illustrates the characteristic topographies and features of different fracture surfaces resulting from tests where the fracture conditions were known. It is not intended to make a complete survey of the published work on microfractography; however, the outstanding contribution of Crussard, Plateau, and Henry (2, 3) should be mentioned.

II. MECHANISMS OF FRACTURE

Fracture Paths

Under a large tensile stress the atoms of a perfect crystal may separate theoretically by sliding past one another or they may pull apart. In general, the fracture path in metals and alloys are the result of fracture processes which all stem from these two theoretical mechanisms of crystal rupture. The different fracture paths can be classified as follows:

* The topography of the fracture surface as seen on an electron micrograph can be very confusing. However, a short study of the contrast resulting from shadowing the replica shows that if the direction of shadowing and the type of replica (one step or two steps) are known, the interpretation of the topography is unambiguous. On a given micrograph it is always possible to find the direction of shadowing by looking carefully at the shadows of some small details.

1. Transgranular Fracture

a. Crystallographic Fracture Path

Cleavage Fracture:

Cleavage is defined as the separation of a crystal along certain crystallographic planes. A typical example of a perfect cleavage fracture is the fracture of crystals of mica which split along their weakly bonded planes of atoms. Many other crystalline substances including metals with body-centered cubic or hexagonal structures may fracture by separation normal to crystallographic planes of high atomic density. In the face-centered cubic structure, fracture by normal separation does not appear to be crystallographically controlled but it may take place on a very small scale in planes subjected to maximum tensile stress. The cleavage fracture of the metal crystals is always preceded and accompanied by some plastic deformation.(4) This means that cleavage is not a simple process of separation along atomic planes and some of the fracture features will be related to this small amount of plastic deformation.

Stress-corrosion or Environmental Fracture:

Under the simultaneous action of static stress and exposure to a corrosive environment the fracture of certain alloys such as alpha-brass or stainless steel takes place along well defined crystallographic planes.

b. Non-crystallographic Fracture Path: Plastic Fracture

Fracture by Uninterrupted Plastic Deformation:

Metals that do not work harden much, some single crystals, and also some polycrystalline metals draw down almost to a chisel edge or a point before breaking apart; this can hardly be termed "fracture" in the normal sense. It is usually referred to as "rupture" because the process arises from prolonged shear on slip planes within the worked region of the crystals which at one point finally shear apart.

Fracture by Formation and Coalescence of Microvoids:

In most of the ductile tensile fractures the reduction of area does not reach 100% although the overall deformation before fracture may be extensive. This is due to the fact that there is formation and coalescence of microvoids in the necked down region of the test specimen. The coalescence of the voids takes place by a process of internal and localized necking. It was observed by electron fractography that this process of plastic fracture by formation and coalescence of microvoids is very common in metals. It has been referred to as a "ductile fracture" (and also a "dimple fracture") in opposition to the

brittle cleavage fracture. The expression "ductile fracture" leads to some confusion since numerous fractures which would be referred to as "brittle fracture" after a macroscopic identification (no overall deformation, low impact energy) are found to be the result of a plastic rupture when they are carefully studied by electron microscopy. In the following discussion, the term "plastic fracture" will refer to a fracture which results from the growth and coalescence of transgranular voids.

2. Intercrystalline Fracture

The two preceding mechanisms of fracture are observed in single crystals and polycrystalline materials; in all cases the fracture is transcrystalline. Polycrystalline materials and multiphase alloys exhibit another mechanism of fracture which is the separation of crystals from each other along the grain or phase boundaries. This is a distinct type of fracture as it does not involve the fracture of the actual crystals; it is referred to as an "intercrystalline fracture" or "phase separation".

Ductile and Brittle Fractures

In practice, it is rare when the fracture surface of a polycrystalline metal exhibits only one of the preceding mechanisms of fracture; usually, one mechanism is predominant, but any of the others may have played a role in the initiation and propagation of the fracture. Consequently, the types of fracture are usually classified according to their cause and their appearance. This classification separates the fractures into two classes, "ductile fractures" and "brittle fractures", according to the amount of deformation and distortion which is present in the neighborhood of the fracture surfaces.

Two types of ductile fractures are usually encountered:

a. A fibrous fracture occurs when the fracture surface is normal to the direction of maximum tensile stress.

b. A shear fracture takes place when the fracture surface makes approximately an angle of 45° with the direction of the maximum tensile stress.

The expression "brittle fracture" covers the following mechanisms and causes of fracture: cleavage, intergranular fracture, phase separation, and environmental fracture.

Fatigue fracture is another type of brittle fracture; it is characterized by a smooth fracture surface with well defined macroscopic and microscopic striations also called crack front arrest lines. Fatigue fracture is usually transgranular but the mechanism of fatigue fracture is not well understood.

It should be repeated again that the expression "brittle fracture", as

it is commonly used, refers to a fracture which occurs without detectable macroscopic deformation. The use of the electron microscope shows that many fractures classified as "brittle" are in fact, the result of a localized plastic rupture as defined previously. A proper re-evaluation of the fracture vocabulary and classifications will be needed in order to keep up with the progress and understanding which result from the use of more sophisticated means of investigation.

The fracture mechanisms selected for discussion in this paper are presented as follows:

(1) cleavage, (2) microvoid coalescence, (3) intergranular fracture and (4) fatigue.

III. CLEAVAGE FRACTURE

The best example of a cleavage fracture is the fracture of alkali halide single crystals such as sodium chloride or lithium fluoride. One would expect the two surfaces created to be perfectly plane, but a single crystal is never perfect and the cleavage crack does not follow a single crystallographic plane. It is broken up along many cleavage planes. The steps between the different planes form a river pattern often called "river markings" which is characteristic of a cleavage fracture. The river lines tend to run together, giving the local direction of crack propagation, either cancelling each other or producing a larger cleavage step. The screw dislocations present in the crystal or created by plastic deformation at the tip of the crack are thought to be responsible for the formation of cleavage steps on the crack surface, but Orowan (5) has suggested that the rivers may be the result of a local twist or shear stress component. This explanation seems to be more plausible because the height of the cleavage steps (Figure 1) would require a large concentration of screw dislocations. Orowan's suggestion has been tentatively confirmed by the fact that low temperature cleavage fracture of annealed and prestrained (room temperature - 8%) low carbon steel shows no marked variation in river density or step heights. The steps or "river markings" between each cleavage surface are often the result of a fracture along a secondary cleavage plane. However, in many cases, when there is a small amount of plastic deformation associated with cleavage the river markings correspond to tear ridges formed by shear. (6)

In the case of polycrystalline materials the orientation of the cleavage plane changes across the grain boundary from one grain to the other. If the orientation change is not too large the crack front crosses the boundary with no change except for the appearance of large cleavage steps originating at the boundary. This is well illustrated at the boundaries EF and GH on Figure 2. When two adjacent grains have a large orientation difference the crack front very often follows the grain boundary in order to go from one cleavage direction to another. Crussard (2) has shown that in polycrystalline aggregates cleavage fracture is a discontinuous process, many different cleavage cracks being nucleated ahead of the main crack and often propagating in opposite directions in adjacent grains.

The junction of these microcracks with the main crack front takes place by cleavage along secondary cleavage planes or separation along grain boundaries. In a polycrystalline aggregate, it also happens that some grains are so poorly oriented for cleavage that they deform extensively and fail by plastic rupture.

Figures 1 and 2 illustrate the cleavage fracture of an Alnico alloy.

Figure 3 represents the cleavage fracture surface of a Charpy impact bar of a low carbon steel broken at 78°K. These three figures illustrate most of the main features of a cleavage fracture:

1. Change of orientation and direction of the cleavage plane from one grain to another;

2. Indication of the local direction of crack propagation by the river markings present on each cleavage plane;

3. Regions of high deformation and/or of intergranular fracture along the grain boundaries;

4. Presence of small cleavage facets or "tongues" on the fracture surface of the steel specimen. The facets are due to the cleavage of deformation twins formed by plastic deformation at the tip of the propagating crack.

In many materials the cleavage facets are not equiaxed but are elongated in the direction of crack propagation. This results in a feather-like appearance of the fracture surface as shown on Figure 4.

IV. PLASTIC FRACTURE-COALESENCE OF MICROVOIDS

As it was pointed out in the preceding classification of the different modes of fracture, a plastic fracture is the result of the growth and coalescence of microvoids formed during the last stages of deformation and during crack propagation. These microvoids produce the numerous concave depressions observed on the two opposite faces of the fracture. Crussard and his co-workers (2) were the first to observe these depressions with the electron microscope. They were named "cupules" or "dimples", the word "dimple" being more commonly used. Crussard (3) explains the mechanism of formation of the dimples as follows: "in the course of deformation and as a result of differences in elastic and plastic properties, microcracks are produced around the particles ahead of the main crack". Dimples have been observed on the fracture surface of a large variety of materials.

The dimples are characterized by their shape and their average size. By and large, the shape seems to depend essentially on the conditions of fracture while the size is more a function of the microstructure of the material.

Conditions of Fracture and Shapes of the Dimples

Beachem (7) has recently published an excellent analysis of this problem which had also been studied partially by Crussard (3) and Tiner. (8) It is necessary to distinguish between a normal fracture, a shear fracture and a tear fracture (crack propagation in a plate under plane strain conditions). The sketches of Figure 5 illustrate the different shapes of dimples resulting from the different modes of coalescence of the microvoids.

Normal Plastic Fracture

The maximum principal stress is normal to the fracture surface and the rate of crack propagation is slow. The dimples are equiaxed as shown on sketch 5a and as illustrated on Figure 6. In many cases a particle, inclusion or precipitate, is observed near the bottom of the dimple where the void was nucleated.

Shear Plastic Fracture

When the state of stress is such that extensive shear takes place by plastic deformation during the formation and coalescence of the microcavities, the dimples are elongated and have the shape of parabola pointing in the direction of shear on each fracture surface. This is illustrated on sketch 5b and Figure 7. A shear fracture surface also shows, besides regions covered with elongated dimples, some very flat areas. According to Crussard, (3) these flat areas are due to fracture along slip planes which have been weakened by deformation. This hypothesis needs further confirmation.

Plastic Fracture by Tear

Sketch 5c shows the formation and orientation of the dimples in the case of a tear fracture. Like in a shear fracture, the dimples have the shape of parabola, but now on both surfaces they point in the direction opposite to the direction of crack propagation. A good example of tear dimples is shown on Figure 8.

Beachem (7) considers that the elongated shape of the dimples is due to the extensive plastic deformation taking place when the microcracks link up with the main crack front. Although this factor plays an important role, it is felt that the parabolic shape of the dimples is the result of a difference in the rates of propagation of the microcracks along the longitudinal and transverse directions of the parabola. This shape can also be explained simply by the fact that the part of the microcrack which is the farthest away from the crack front, would have more time to propagate in a transverse direction than the part closes to the main front. It is interesting to note that similar parabola-shaped dimples appear on the fracture surfaces of non-crystalline materials such as lucite or plexiglass as shown on Figure 9. In this case, however, the dimples are very large, probably because of the limited number of crack nucleation sites present ahead of the main front. Irwin (9)

showed that the macroscopic markings on a fracture surface are the result of the differences in the speed of propagation of a multitude of separately initiated components of fracture. The same phenomena seem to take place on a microscopic scale in the process of ductile fracture of metals and alloys. The shape and size of the dimples will, therefore, depend on the overall velocity of propagation of the main crack front which is, in turn, governed by the rate and distance at which advance initiations can occur and the rapidity with which the microcracks can be linked together.

Size of Dimples

The second phase particles and inclusions distributed in a metal or alloy play an important role in the initiation of the microcracks and, therefore, in the mechanism of fracture. This is confirmed by the fact that very pure and clean metals, solid solutions and even quenched supersaturated solid solutions such as Al-Cu when pulled in tension break with 100 per cent reduction in area. This role of the second phase particle initiating fracture, explains why there is a relationship between the size and distribution of the particles and ductility or reduction of area. Plateau (10) has recently derived a mathematical expression for this relationship and has shown that a large amount of experimental data fits his theoretical curve but so far no relationship between the size of the dimples and the interparticle spacing has been established. This would be rather difficult because of the complex shape of the dimples and only a statistical distribution of sizes would be meaningful.

Figures 10, 11 and 12 illustrate the different sizes and shapes of dimples observed in some common materials. In age hardening alloys such as the aluminum alloys or the maraging steels where most of the second phase particles are very small (smaller than 500A), it is evident that the size of the dimples is much larger than the spacing between the precipitates. This shows that only a limited number of inclusions or precipitates act as crack nucleation sites ahead of the main crack front, and that this number depends on the overall velocity of propagation of the crack. Irwin (9) concludes from his observations that an increase in crack velocity is accompanied by an increase in the number of microcracks which are initiated closer and closer to the main crack front.

In steels such as 4340, it has been observed that the higher the fracture toughness, the larger the dimples. This is explained by the fact that the size of the dimples is going to depend on the amount of plastic growth taking place before the voids coalesce. The work hardening behavior of the surrounding matrix will in turn be the controlling factor of plastic growth. In this connection it was shown (7) that not only the size but also the depth of dimples increase with the test temperature in the brittle-ductile temperature transition of steel.

Finally, Rogers (11) pointed out that inclusions are not necessarily the only sites of initiation of microvoids in a plastic fracture.

Microcracks may form at dislocation pile-ups or certainly along subboundaries. The smooth, slightly polyhedral dimples observed in 70-30 brass on Figure 12 may result from decohesion along a slip plane or a subboundary. Dimples may also be initiated at grain boundaries, but it is, in general, impossible to distinguish the grain boundaries and the grain size on a fracture surface showing extensive dimple formation. However, in titanium alloys the dimple size has been observed in many cases to approach the grain size.

V. INTERGRANULAR FRACTURE

Intergranular fracture is a separation of the crystals from each other along the grain boundaries. Figure 13 is a typical intergranular fracture in a 4340 steel. The grain boundary facets are slightly curved which show that the conditions for metastable equilibrium of the grain boundary network were satisfied at the austenitizing temperature. The small "hairlines" on each facet are unaccounted for and may be related to the second phase particles or to the mechanism of separation of the grains. Another example of a perfect intergranular fracture is shown on Figure 14 which represents the fatigue fracture surface of a 70-30 brass.

All these figures are good illustrations of a brittle intergranular fracture, the term "brittle" referring to the lace of deformation associated with the final separation of the grains. This type of fracture is observed at room temperature in materials where the grain boundaries may have been embrittled by a film of a brittle phase or by the segregation of an impurity without the appearance of a second phase. This seems to be the case of the temper brittleness and hydrogen embrittlement of high strength steels. Stress corrosion fracture in steels and aluminum alloys is usually intergranular; but in most cases, the fracture surface is so badly corroded that a detailed identification of fracture features is usually very difficult.

The best known examples of intergranular fracture are the result of creep at temperatures above the equicohesive temperature (0.5 absolute melting point). In opposition to creep fracture, it should be mentioned that Backofen (12) has recently observed intergranular fracture in pure aluminum at very low temperatures, which would indicate the existence of another equicohesive temperature. Although grain boundary cracking corresponds in general to a slow rate of crack propagation, it has not been possible so far to determine the exact mechanisms of crack propagation. There are no clearly visible features such as crack front arrest lines or nucleation sites. Some controversial microcavities, supposedly due to hydrogen condensation, have been observed in some cases in steels.(13)

Grain boundary fracture is not always a perfect brittle separation along the grain boundary planes. It can also take place by the preferential formation and coalescence of microvoids along the grain boundaries. This type of fracture is referred to as a plastic intergranular fracture. This type of fracture is usually connected with the well known delamination fracture of some aluminum alloys which result from the depletion

of second phase precipitates along the grain boundaries. Figure 15 shows an example of this type of grain boundary fracture. Another example of plastic intergranular fracture takes place during creep at high temperatures when voids form along grain boundaries by diffusion of vacancies.

In the case of high strength steels, intergranular fracture always follows the prior austenite grain boundaries. In the same material it is found that very often, regions of transgranular fracture by microvoid coalescence are mixed in a region of intergranular cracking. A good exmple of this juxtaposition of two mechanisms of fracture is shown on Figure 16. The ratio of intergranular cracking to microvoid coalescence has been shown in steels to depend upon the rate of crack propagation, that is slow versus fast fracture.

A fracture surface similar to an intergranular fracture is usually found in multiphase materials when the fracture path follows the interface between the different phases. This is the case for grey cast iron. The topography of the fracture surface represents the three-dimensional shapes of the different phase constituents. The constituents can be easily identified on the fracture surface if their average size and shape on a cross section are known.

VI. FATIGUE FRACTURE

The examination of the fatigue fracture surface of an aluminum alloy by optical microscopy shows dull and bright regions. The dull zones are depressions usually with a large inclusion visible at the bottom of the depression. The bright zones show a series of regular striations as illustrated by Figure 17. The examination of the same surface by electron microscopy shows that the depressions are made up of dimples characteristic of a rapid, plastic fracture. The striations of the bright zones are clearly resolved (Figure 18) and in the case of a fatigue test under a constant stress level, the spacing of the striations is locally very uniform. The examination of program loaded fatigue fractures has demonstrated that each of the characteristic fatigue striations first observed by Zapffe and Worden (14) is produced by a single cycle of stress, (15) thus the striations also called crack front arrest lines, represent the successive positions of a transgranular front at each load cycle.

Forsyth (16) has recently given an excellent survey of the mechanisms of fatigue crack propagation in aluminum alloys. Two general types of striations have been recognized, the brittle and the ductile types. Figure 19 taken from Forsyth, illustrates the differences between the two types of striations. The brittle striations are connected with what seems to be a cleavage fracture along sharply defined facets. Numerous river line markings separating these facets run normal to the striations as shown in Figure 20. The profile of a brittle striation is shown in the sketch Figure 19d. As far as it is known, brittle striations have been observed only in high strength aluminum alloys, and they are often associated with the presence of a corrosive media. However, it is possible to produce ductile and brittle striations in adjacent

areas where the governing factor is the stress state. Figure 17 shows the characteristic flat facet of brittle fatigue cracking with ductile striations on either side. Sections normal to the crack propagation direction, Figure 21, and sterographic observations show that the flat facets are always normal to the tensile axis while the ductile striations occur on inclined planes, Figure 22. Figure 21 also shows that the orientation of the fracture plane varies from grain to grain. The direction of crack propagation in Figure 17 shows that the rate of crack propagation also varies from grain to grain.

The more common ductile striations have also been observed in polymers which would show that their formation is not necessarily related to the crystallographic nature of metals. The exact mechanism of formation of these striations is not clearly understood. Sketch 19c presents different profiles of fatigue striations. Smith and Laird (17) and McEvily (18) have shown that in the case of high stress fatigue, the profiles of the two fracture surfaces do not match. Under conditions of low stress fatigue, it is not clear at this stage, whether the profiles are of the type II or type III represented in Figure 19. It does appear, however, that striation formation occurs in two steps, and that one increment of growth occurs on the closing mode of the stress cycle. In a spectrum load test a series of six major load cycles were preceded and followed by large numbers of lower load cycles. The general loading spectrum is shown in Figure 23. It will be noted that a major closing precedes each high load block. In Figure 24 the fractographic record of the loading sequence is shown. The crack propagation direction is as indicated and it will be noted that the set of major load striations is preceded by a broad flat band. This band can only be the result of crack extension on the closing mode. Consequently, this suggests that fatigue cracking and ductile striation formation are controlled on a microscale by a reversible shear mechanism.

Grain boundaries play an important role in fatigue crack propagation. The different figures presented here show that in aluminum alloys, the crack front is held up along grain boundaries, and the orientation of the striations changes from one grain to the other. This could be accounted for by the fact that in high stacking fault energy materials, fatigue cracking is influenced by the amount of cross-slip which will be more extensive in the material adjacent to grain boundaries. In materials of lower stacking fault energy (nickel alloys, brass) the crack front is straight across a given grain showing that the grain boundary has little retarding effect.

Under uniform load, the height and the spacing of the striations increase with the crack length. Crack growth rates have been shown to be a function of stress amplitude (19) and mean stress. (20) Fatigue crack propagation lends itself nicely to a fracture mechanics treatment where the controlling factor is the stress intensity K_{I} determined form equations of the type $K_{Ii} = \sigma_g \sqrt{\pi a}\,\alpha$ Where:

σ_g = gross area stress

a = one half the crack length (center notched panel)

α = crack length to specimen width correction factor

Data reporting crack growth rates $\frac{da}{dN}$ as a function of stress intensity are readily available in the literature. (21) A basic discrepancy between growth rates determined by surface optical techniques and electron fractographic means has been reported by Pelloux. (22) If the crack front does not move in a uniform manner over its whole length, common for K_{II} values, the average spacing of the striations will be larger than the macroscopic growth rate. However, at higher K_{II} values brittle fracture of inclusions and ductile tearing around these inclusions results in a rapid local advance of the crack front. Consequently, the striation spacing is, in general, smaller than the macroscopic crack growth rate observed on the surface of a test panel. Figure 18 illustrates clearly the extensive brittle fracture of large inclusions.

The fracture topography of a fatigue failure provides the most complete history of the loading pattern available to the engineer. The local stress intensity and the local inherent toughness of the material are indicated at each growth increment. How to successfully interpret the surface markings has been the subject of extensive fatigue investigations at The Boeing Company. It has been established that the loading sequence for non-uniform load application can greatly influence the striation spacing, but for tension - tension tests there is evidence that each stress cycle of a spectrum load application results in some growth. However, smaller growth increments are not always resolved in the electron microscope, Figure 25. This problem may be resolved from an engineering point of view by using an equivalent damage concept to define the loading spectrum.

As an example, the loading spectrum shown in Figure 26 was applied to a complex component and the fractographic record, Figure 27 was obtained from the fracture face. It is now possible to produce an equivalent damage spectrum utilizing the growth rate data from the photograph, $\frac{da}{dN}$ vs. K_{II} data obtained experimentally and the appropriate stress intensity equation. The cumulative damage due to the eight lower load cycles is combined with the first major growth increment and the total equivalent damage spectrum is as shown in Figure 26.

In general, the striations in different materials are not as sharply defined as they are in high strength aluminum alloys. In steels for instance, the successive positions of the crack front do not appear clearly defined; the striations are short and discontinuous. When compressive components are included in the stress cycle, the details of the fracture surface may be destroyed by the rubbing action of the two fracture faces. This is often the case with service failure where a fatigue mode of fracture is identified by the presence of a few striations on a flat surface and the absence of other characteristic fracture features. Crack propagation under cyclic load is not always transgranular with a striated appearance. In some cases, fatigue cracks have been observed to propagate along grain boundaries. 70-30 brass was already given as an example of this type of behavior which can also take place in steels.

VII. CONCLUSION

In summary this short review shows that the fracture surfaces of metals and alloys exhibit markings and a topography which are characteristic of the mechanisms of fracture operating during the initiation and the propagation of the crack. These markings can be easily and best differentiated by electron microscopy.

The different types of fracture are separated into two classes depending upon the fracture path:

- intergranular fracture and transgranular fracture.

Figure 28 illustrates in conclusion, the different profiles of the fracture surfaces which result from the different mechanisms of fracture. Transgranular fracture takes place either:

- by separation along crystallographic planes in the case of cleavage and stress corrosion,
- or by the formation and coalescence of microvoids which leave concave depressions called "dimples" on both surfaces of the fracture. This mechanism of fracture is essentially non-crystallographic in nature,
- or by the slow progression of a crack front under cyclic loads. A transgranular fatigue crack seems to be only partially controlled by the crystalline nature of metals.

Intergranular fracture is either:

- brittle when it is the result of a perfect separation of the grains along the grain boundary planes,
- or ductile when this separation is associated with the plastic formation of voids along the grain boundaries.

In general, one, two, or more of these mechanisms of fracture may be juxtaposed on a given fracture surface according to the nature of the material and the fracture conditions.

The results obtained so far by the techniques of electron fractography show the great possibilities offered by using the electron microscope to study fracture surfaces. In the analysis of service failures these techniques have been, and are today, a most valuable tool. It is now possible to determine on a microscale the local modes of fracture, the main origin and the sites of secondary crack initiation and also to follow the direction of crack propagation. The influence of metal defects, second phase particles, grain boundaries, etc., on the initiation and propagation of the crack can be studied directly and easily at high magnifications.

Although electron fractography is becoming a common tool among the

metallurgical laboratory techniques, a large amount of research remains to be done in order to get a complete understanding of the mechanisms of fracture which lead to the formation of fracture surface markings. So far, this research has been, in general, limited to a purely qualitative evaluation and classification of the modes of fracture. It is time now to try to relate the size, shape and distribution of the fracture features to the quantitative measurements of fracture properties such as fracture strength, toughness and ductility. This research should have a very high yield to investment ratio, the replicating techniques are simple, reliable and cheap; the electron microscopy work does not require a high resolving power and can be carried out with the less sophisticated electron microscopes. Finally, there will be a lot of fractures available for a long time.

ACKNOWLEDGMENTS

The authors would like to express their gratitude to Mrs. A. Raisanen, Miss U. Stark, D. E. Austin, D. H. Pasley, J. Mavic, and J. Rutkiewicz

REFERENCES

1. C. A. Zapffe and M. Clogg, Trans. Am. Soc. Metals, 34, 71 (1945)

2. C. Crussard, R. Boroine, J. Plateau, Y. Morillon and F. Matray, J. Iron Steel Inst. (London), 183, 146 (1956)

3. C. Crussard, J. Plateau, R. Tamhankar, G. Henry and D. Lajeunesse, A Comparison of Ductile and Fatigue Fractures, Fracture Swampscott Conf., (1959), John Wiley and Sons.

4. H. Schordin, Velocity Effects in Fracture, Fracture Swampscott Conf., (1959) John Wiley and Sons.

5. E. Orowan, Private Communication, 1965.

6. C. D. Beachem, B. F. Brown, A. J. Edwards, NRL Memorandum Reports 1432, June 1963

7. C. D. Beachem, Transactions ASM, 56, 318, (1962).

8. N. A. Tiner, Am. Soc. for Test. Mat., 82 (1961).

9. J. A. Kies, A. M. Sullivan, G. R. Irwin, J. Appl. Phys. 21, 716 (1950).

10. J. Gurland, J. Plateau, Trans. ASM, 56, 442 (1963)

11. H. C. Rogers, Trans. Met. Soc. AIME 218, 504 (1960).

12. G. Y. Chin, W. F. Hosford, W. A. Backofen, M.I.T. Reprint 16C-184 Metallurgy Department.

13. A. Phillips and G. Bennett, Metal Progress, Vo. 79, 5, 97 (1961).

14. C. Zapfee and C. Worden, Trans. ASM, 43, 958 (1951)

15. P. Forsyth and D. Ryder, Aircraft Engineering, 32, 96 (1960)

16. P. J. E. Forsyth, Acta. Met. 11, 703 (1963).

17. C. Laird, G. C. Smith, Phil. Mag. 7, 847 (1962).

18. A. J. McEvily, R. C. Boettner, T. L. Johnston paper presented at the 10th Sagamore Army Materials Research Symposium

19. P. C. Paris, The Growth of Cracks Due to Variations in Load, Doctorial Dissertation, Lehigh University, (1962).

20. D. Broek and J. Schijve, National Lucht - en Ruimtevaartlaboratorium Report, NLR-TN M.2111, January 1963

21. D. R. Donaldson and W. E. Anderson, Crack Propagation Behavior of Some Airframe Materials, Crack Propagation Symposium, Cranfield England, September 27, 1961.

22. R. M. N. Pelloux, Boeing Scientific Research Laboratories Report, D1-82-0297, September 1963.

Figure 1 - CLEAVAGE FRACTURE - Typical river markings on a cleavage plane in an Alnico alloy. The river markings along ABC probably originate at a subboundary. 3600X

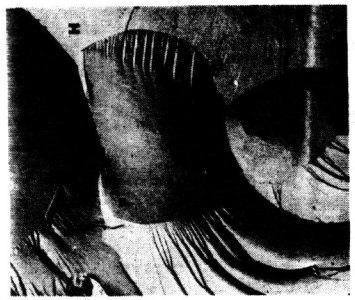

Figure 2 - CLEAVAGE FRACTURE - Typical cleavage fracture through many grains of an Alnico alloy. The grain boundaries EF and GH are clearly at the origin of the formation of river markings. In grains A and B fracture was intercrystalline. 3400X

Figure 3 - CLEAVAGE FRACTURE - Fracture surface of a low carbon steel broken by impact at 78° K. ABC is a grain boundary; BD is a typical river marking. The facet F is due to the cleavage of a deformation twin. Fracture in G is intergranular. 3200X

Figure 4 - CLEAVAGE FRACTURE - Cleavage fracture in a TZM molybdenum alloy. The large cleavage "feathers" are made up of many cleavage facets. Extensive tear takes place between the large regions of cleavage. 3800X

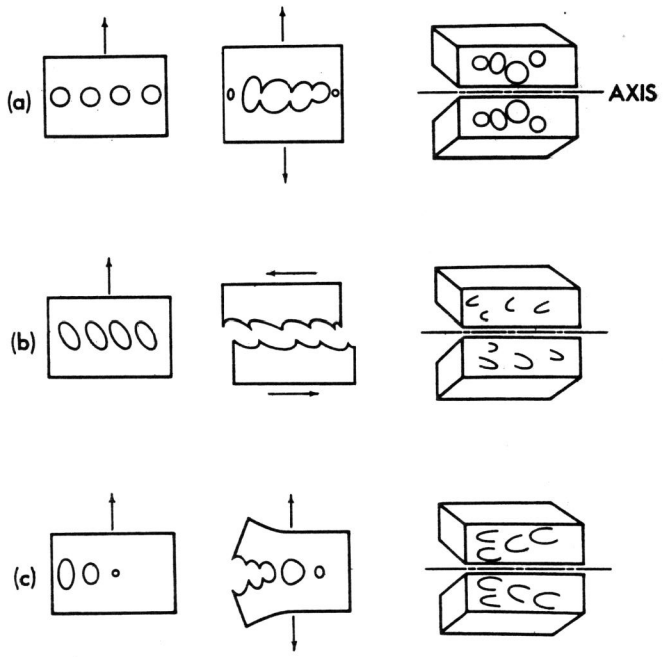

Figure 5 - PLASTIC FRACTURE
a - normal plastic: formation of round dimples
b - shear plastic: formation of elongated dimples pointing in the direction of shear on each fracture surface,
c - tear plastic: formation of elongated dimples pointing in the direction opposite to the direction of each propagation.

Figure 6 - PLASTIC FRACTURE - NORMAL MODE - Formation of round, equiaxed dimples in a normal plastic fracture of 4340 steel. Some inclusions or second phase particles can be observed at the bottom of the dimples.
2800X.

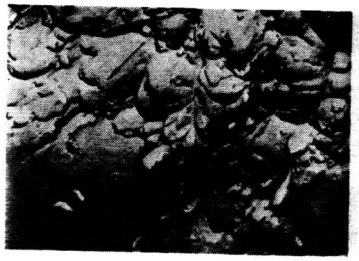

Figure 7 - PLASTIC FRACTURE - SHEAR MODE - Formation of elongated dimples and of a flat region of glide decohesion in a shear fracture of a 4340 steel. The arrow indicates the shear direction. 2400X.

Figure 8 - PLASTIC FRACTURE - TEAR MODE - Elongated dimples resulting from a tear plastic fracture in a 4340 steel. See Sketch 5c. 3000X

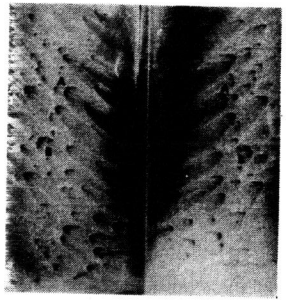

Figure 9 - FRACTURE MARKINGS ON PLEXIGLASS.- Matching fracture surfaces. Note the matching features A, A' and B, B' on the two fracture faces. The parabola markings are similar to the plastic dimples observed in a tear ductile fracture of a metallic material. 2.6X

Figure 10 - PLASTIC FRACTURE - Example of tear plastic dimples in a 7178 aluminum alloy. The average size of the dimple is of the order of microns.
3000X

Figure 11 - PLASTIC FRACTURE - Example of plastic dimples in a 2219 aluminum alloy. Note the range of sizes of dimples.
3600X

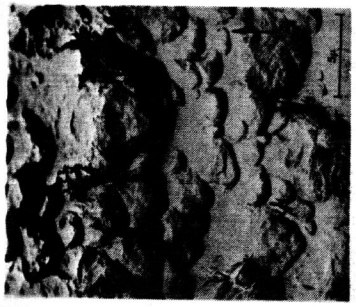

Figure 12 - PLASTIC FRACTURE - Large dimples in a 70-30 brass resulting from a tear fracture. Many of the dimples may have originated at dislocation pile-ups or sub-boundaries.
5000X

Figure 13 - INTERGRANULAR FRACTURE - Brittle intergranular fracture in a 4340 steel. This intergranular fracture at the origin of a service failure was probably due to stress corrosion or hydrogen embrittlement. Note the hairlines along the grain boundaries facets and the microcavities in A and B. 3000X.

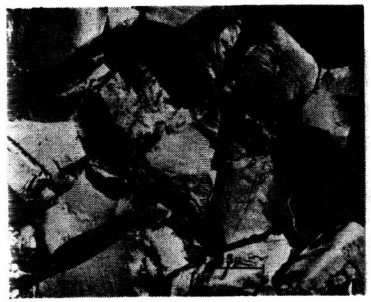

Figure 14 - INTERGRANULAR FRACTURE - Brittle intergranular fracture in a 70-30 brass. This fracture is the result of a slow crack propagation under cyclic load in a centrally notched panel of brass. 3000X

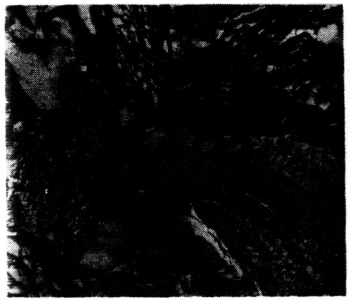

Figure 15 - INTERGRANULAR FRACTURE - Plastic intergranular fracture in a 2219 alloy. The difference in orientation of the grain boundary facets is well marked and the shear direction is given by the direction of elongation of the dimples. 3500X

Figure 16 - MIXED PLASTIC - INTERGRANULAR FRACTURE Example of juxtaposition of two modes of fracture: plastic and intergranular in a 4340 steel. 2500X

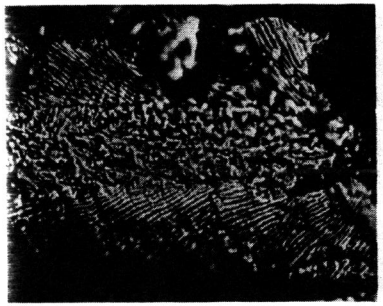

Figure 17 - FATIGUE FRACTURE - Optical micrograph of a fatigue fracture in a 7178 aluminum alloy. The regions out of focus are due to the small depth of field of the optical microscope. 1000X

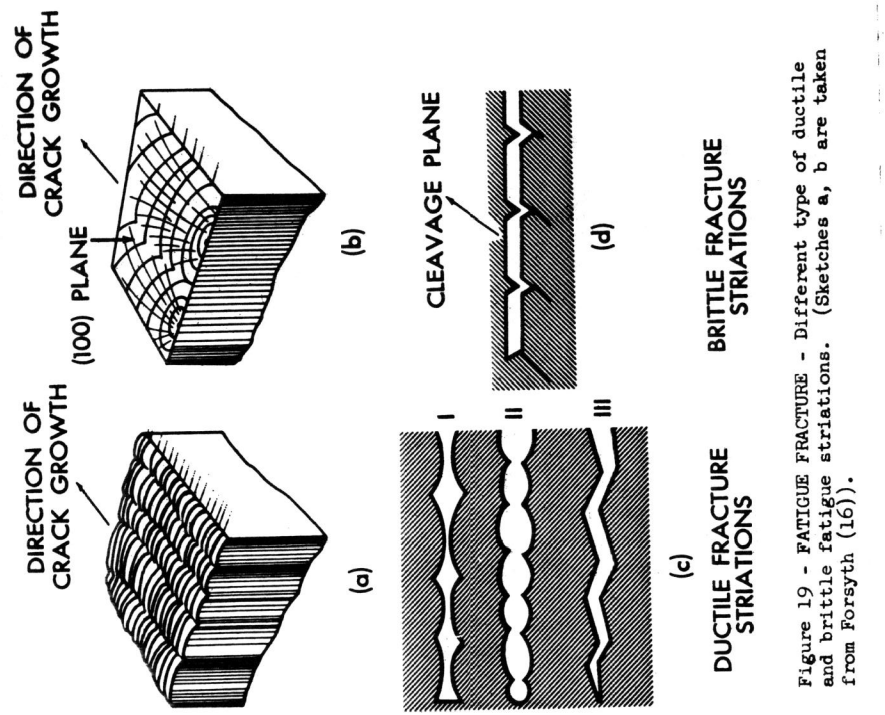

Figure 19 - FATIGUE FRACTURE - Different type of ductile and brittle fatigue striations. (Sketches a, b are taken from Forsyth (16)).

Figure 18 - FATIGUE FRACTURE - Examples of ductile fatigue striations and brittle fracture of second phase particles in a 7178 aluminum alloy. 3500X

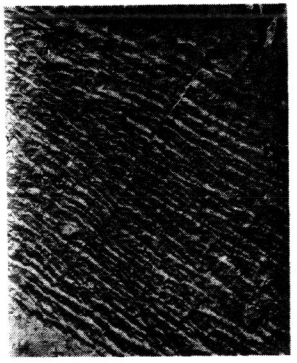

Figure 20 - FATIGUE FRACTURE - Example of brittle fatigue striations in a service failure of a 2014 aluminum alloy. Note the cleavage facets running parallel to the direction of crack propagation and normal to the fatigue striations. 3000X.

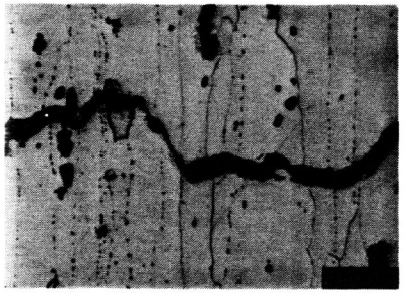

Figure 21 - FATIGUE FRACTURE - The section is normal to the crack propagation direction in a 7178 aluminum alloy. Brittle striations occur on the horizontal and ductile striations on the inclined segments.

520X

Figure 22 - FATIGUE FRACTURE - Ductile and brittle striations in a 7178 aluminum alloy occur in adjacent areas, but only the ductile striations are clearly defined. 2200X

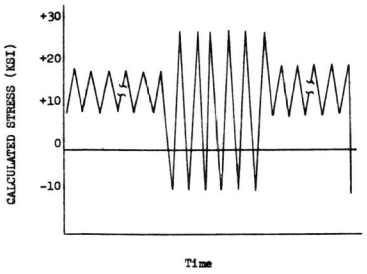

Figure 23 - CYCLIC LOAD SPECTRUM - This loading spectrum was used to produce the fracture topography shown in Figure 24.

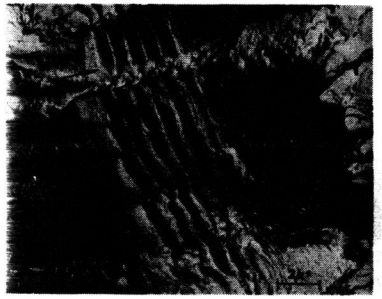

Figure 24 - FATIGUE FRACTURE - This 7075 aluminum alloy fracture topography from a spectrum load test indicate that the major growth increment occurred on the major closing prior to the first maximum load. 5000 X

Figure 25 - FATIGUE FRACTURE - Three distinct growth bands are apparent in the fracture topography of this spectrum loaded 7178 aluminum alloy. Loading in this spectrum was divided into three general load levels. Even though striations are not clearly defined in each area, some growth did occur. 2200X.

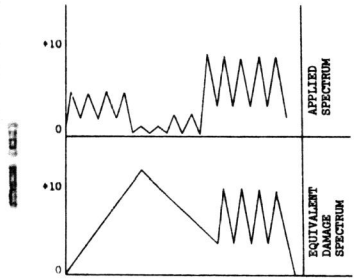

Figure 26 - CYCLIC LOAD SPECTRUMS - The spectrum loads actually applied to a 7079 aluminum alloy are shown above an equivalent damage spectrum can be drawn utilizing the crack growth information recorded on the fracture surface seen in Figure 27.

Figure 27 - FATIGUE FRACTURE - The applied spectrum loads shown in Figure 26 produced this fracture topography.

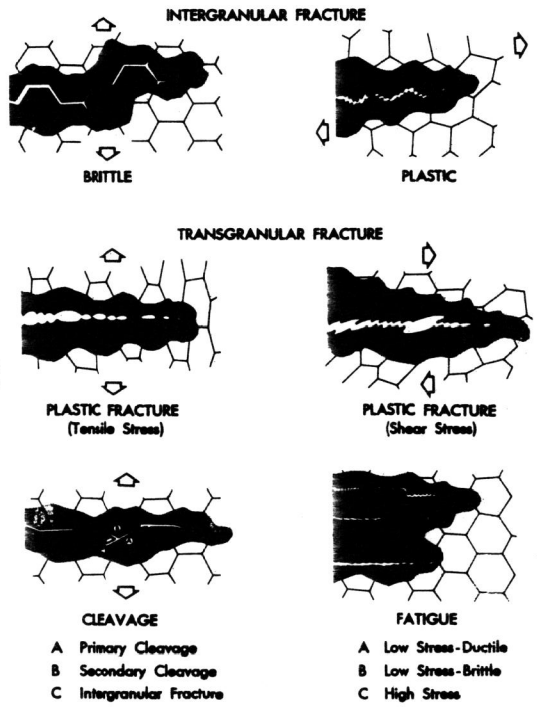

Figure 28 - FRACTURE PATHS. Sketches a to f represent the characteristic profiles of the different fracture paths observed in most metals and alloys.